The ultra-high-energy cosmic-ray sky above 32 EeV viewed from the Pierre Auger Observatory

Jonathan Biteau[a,*] **on behalf of the Pierre Auger**[b] **Collaboration**
(a complete list of authors can be found at the end of the proceedings)

[a] *Université Paris-Saclay, CNRS/IN2P3, IJCLab, 91405 Orsay, France*
[b] *Observatorio Pierre Auger, Av. San Martín Norte 304, 5613 Malargüe, Argentina*

  E-mail: spokespersons@auger.org

The region of the toe in the cosmic-ray spectrum, located at about 45 EeV by the Pierre Auger Collaboration, is of primary interest in the search for the origin of ultra-high energy cosmic rays (UHECRs). The suppression of the flux with increasing energy can be explained by the interaction of UHECRs with intergalactic photons, resulting in a shrinking of the observable universe, and/or by cut-offs in acceleration potential at the astrophysical sources, yielding a high-rigidity sample of single (or few) UHECR species around the toe. The predominance of foreground sources combined with reduced deflections could thus offer a path towards localizing ultra-high energy accelerators, through the study of UHECR arrival directions. In this contribution, we present the results of blind and astrophysically-motivated searches for anisotropies with data collected above 32 EeV during the first phase of the Pierre Auger Observatory, i.e. prior to the AugerPrime upgrade, for an exposure of over 120,000 km^2 yr sr. We have conducted model-independent searches for overdensities at small and intermediate angular scales, correlation studies with several astrophysical structures, and cross-correlation analyses with catalogs of candidate extragalactic sources. These analyses provide the most important evidence to date for anisotropy in UHECR arrival directions around the toe as measured from a single observatory.

---

*Presenter

1. The Southern sky at ultra-high energies

The night sky is full of marvels. At the high-energy frontier, beyond EeV ($\equiv 10^{18}$ eV) energies, the night-sky brightness is dominated by ultra-high energy cosmic rays (UHECRs). UHECRs are detected, following their entry in the atmosphere, by sampling with a surface detector the secondary particles resulting from the development of extensive air showers and, during clear moonless nights, through the fluorescence light emitted by nitrogen molecules excited by these secondary charged particles [1]. The surface detector of the Pierre Auger Observatory has enabled an exquisite measurement of the UHECR spectrum [2]: it features a spectral hardening at $5.0 \pm 0.1 \pm 0.8_{\rm sys.}$ EeV, the "ankle", followed by two softenings at $13 \pm 1 \pm 2_{\rm sys.}$ EeV and $46 \pm 3 \pm 6_{\rm sys.}$ EeV, denoted here as the "instep" and the "toe", respectively. UHECRs above the ankle have long been thought to be of extragalactic origin, based on the spectral hardening which suggests an origin distinct from the lower energy spectral component. Such an extragalactic origin was recently confirmed by the discovery of a large-scale deviation from isotropy [3]. This discovery is driven by a first-harmonic modulation in right-ascension in the instep region, between 8 and 16 EeV, which is well modeled by a dipole of amplitude $6.3^{+1.3}_{-0.9}$ % (with a p-value of 3.1×10^{-7}) growing with energy up to 10 and 16% in the energy ranges $16 - 32$ EeV and ≥ 32 EeV, respectively [4]. The reduced event counts weakens the p-values in these two higher energy ranges (7×10^{-4} and 1%, respectively).

UHECR data collected above the ankle at the Pierre Auger Observatory are best described by a mix of nuclear species, ranging from protons to nuclei at least as massive C-N-O. Both the spectrum and mass-dependent observables fit within a scenario where nuclei are accelerated up to a rigidity $R \equiv E/Z \approx 5$ EV [2], where E and Z are the energy and charge of the nucleus. The by-products of He nuclei are thus expected to dominate the instep region while those of C-N-O nuclei would dominate the toe region. He and C-N-O nuclei travel to the Earth across limited distances, characterized by a lifetime of ~1 Gyr in the instep region or $10 - 100$ Myrs in the toe region [5]. Such limited lifetimes motivated the comparison of the UHECR dipole in the instep region with the distribution of stellar mass within 140 Mpc from the 2MRS catalog [6]. Both the evolution of the UHECR dipole amplitude and its direction fit within a scenario where UHECR sources follow the distribution of stellar mass traced by 2MRS in the local Universe, accounting for the crucial but still underconstrained deflections in the Galactic magnetic field (see [3] and references therein). Whether all galaxies host UHECR accelerators or sub-categories of hosts are preferred remains to be determined. The toe region may hold crucial clues, as a reduced horizon at these energies could reveal preferred directions or patterns aligned with all or some nearby galaxies.

Here, we re-examine searches for anisotropies [7, 8] above 32 EeV, where the significance of the dipolar signal drops. Revisiting the major searches for small- and intermediate-scale anisotropies performed by the Pierre Auger Collaboration is motivated by the wealth of data accumulated over more than 80% of the sky with the Observatory. The dataset explored in the present work covers 17 years (Jan. 2004 − Dec. 2020) of operation of the surface detector, which is composed of 1,600 stations spread over an area of 3,000 km^2 in the province of Mendoza, Argentina [9].[1] The exposure accumulated up to zenith angles of 80° over this period corresponds to 122,000 km^2 sr yr (vs. 66,000 and 90,000 km^2 sr yr in [7, 8], respectively), with more than 2,600 events above 32 EeV.

---

[1]Despite the pandemic, the surface detector of the Pierre Auger Observatory showed high-reliability throughout 2020: a steady event rate is observed above its full-efficiency energy threshold across the 17 years of operation.

2. Underconstrained searches for anisotropies

Following [7], we start with a blind search for a localized overdensity. The number of events, $N_{observed}$, above an energy threshold E_{th} within a disc of radius Ψ centered on equatorial coordinates (R.A., Dec.) is compared with that expected, $N_{expected}$, from an isotropic distribution of arrival directions accounting for the geometric exposure of the Observatory. The search is performed over a grid, by threshold steps of 1 EeV between 32 and 80 EeV, by radial steps of 1° between 1° and 30°, and on a directional grid of 1° spacing, a value which corresponds to the angular resolution of the Observatory at the energies of interest. Besides searching for the main overdensity in the field of view (FoV) of the Observatory, a search for autocorrelation on specific angular scales offers the possibility to evaluate a coherent clustering in multiple directions. The autocorrelation search is performed over the same threshold grid as the overdensity search and, following [7], pairs of events are counted over a radial grid of 1°-steps from 5° to 30°, with a spacing of 0.25° from 1° to 5°.

The two analyses discussed above are fully model-independent and can be complemented by studies of specific large-scale planar structures, more particularly the supergalactic plane, along which galaxies within a few tens of Mpc are distributed, and the Galactic plane and center which were studied in [7]. The number of free parameters, or alternatively the dimensionality of the grid, is reduced for such analyses as the direction is fixed. The threshold and the angular scale are explored over the same grid as that employed for the autocorrelation search.

Analysis	E_{th} [EeV]	Ψ [deg]	$N_{observed}$	$N_{expected}$	Post-trial p-value
Overdensity	41	24	156	98	1.4×10^{-2}
Autocorrelation	41	11	11,709	11,023	0.21
Supergalactic plane	44	20	395	351	0.16
Galactic plane	58	20	154	132	0.41
Galactic center	64	18	17	10	0.54

Table 1: The results of the searches for a localized overdensity, for autocorrelation of events and for overdensities along the supergalactic plane, Galactic plane and Galactic center. The threshold energy and disc/band radius (pair angular distance for the autocorrelation study) minimizing the probability that the signal arises from isotropy are reported in the second and third columns. The number of events (of pairs for the autocorrelation study) observed and expected above the indicated energy threshold and at the indicated angular distance are reported in the fourth and fifth columns. The last column provides the post-trial p-value accounting for the search over the grid.

The results of the analyses are presented in Table 1. The reported energy threshold and angle are those that minimize the probability that the signal arises from isotropy. The overdensity, autocorrelation and supergalactic plane searches show a maximal excess above similar energy thresholds,[2] close to 40 EeV, while the largest excesses along Galactic structures are found at energy thresholds close to 60 EeV. None of the search yields a notable deviation from isotropy, with significances smaller than 1σ for Galactic searches, autocorrelation and supergalactic plane studies, and about 2.2σ for the search for a localized overdensity.[3]

---

[2]The energy resolution of the surface detector is estimated at $\sim 7\%$ in the energy range of interest [2].

[3]All p-values are converted here into significances as $s = \sqrt{2}\,\mathrm{erfc}^{(-1)}(2p)$.
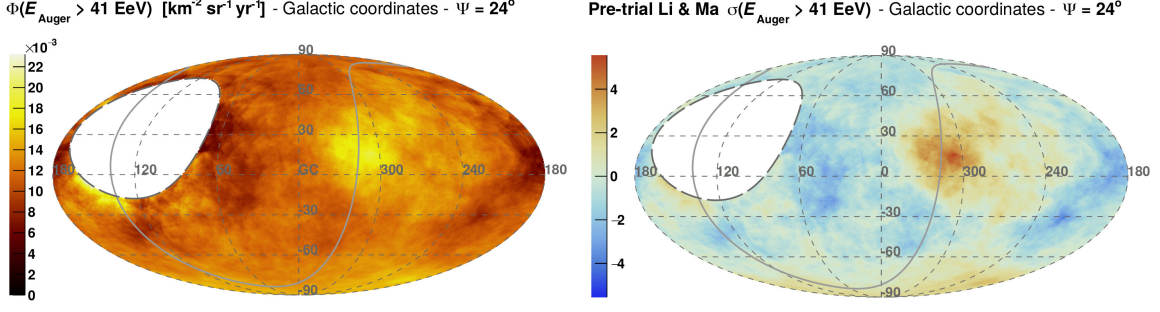
Figure 1: *Left*: The flux map in Galactic coordinates of UHECRs above 41 EeV smoothed with a top-hat profile of radius 24°. *Right*: The associated Li & Ma pre-trial significance map of localized overdensities. The supergalactic plane is shown as a light grey solid line. The edge of the FoV of the Pierre Auger Observatory is shown as a dark grey dashed line.

A further examination of the results of the overdensity search is provided in Fig. 1. The UHECR flux map and pre-trial significance map are displayed in Galactic coordinates following the same procedure as in [10], above an energy threshold of 41 EeV with a top-hat smoothing on angular scale of 24°, which correspond to the values found in the overdensity study. The most significant excess, with a post-trial p-value of 1.4%, is found in the direction $(R.A., Dec.) = (198°, -47°)$, close to the intersection of the Galactic and supergalactic planes at Galactic coordinates $(l, b) \approx (307°, 16°)$.

3. Catalog-based searches for anisotropies

No indication beyond $3\,\sigma$ is found in the searches highlighted in Table 1. These limitations motivate more constrained studies, either in specific areas of the sky or against flux patterns expected from multiwavelength extragalactic observations. A favored area of the sky is the Centaurus region, which has raised interest from the UHECR community since the early days of the Pierre Auger Observatory (see [11], with an exposure equivalent to $\sim 7\%$ of the current one). This region encompasses prominent galaxies from the Council of Giants [12], which consists of galaxies distributed in a disk of $3 - 5$ Mpc radius roughly centered on the Milky Way. These prominent electromagnetic sources are the radio-galaxy Centaurus A at $(l, b) = (309.5°, 19.4°)$ and the starforming galaxies M 83 at $(l, b) = (314.6°, 31.9°)$, Circinus at $(l, b) = (311.3°, -3.8°)$ and NGC 4945 at $(l, b) = (305.3°, 13.3°)$, the latter two also containing a Seyfert nucleus.[4]

An overdensity search dedicated to this region, centered on Centaurus A based on the *a priori* choice adopted by the community, yields a most significant excess of 56 events on top of 120 expected above a threshold energy of 41 EeV and within a radius of 27°, as illustrated in Fig. 2, left. These values are, as expected, comparable to those obtained from the main localized overdensity, although that underconstrained analysis is more penalized by the directional search. With a signal fraction of $4.4 \pm 0.6\%$ relative to all events observed above 41 EeV and a post-trial p-value of 6×10^{-5}, an *a priori* focus on the Centaurus region provides a $3.9\,\sigma$ deviation from isotropy at intermediate angular scales in the toe region.

---

[4]As radio-galaxies, Seyfert galaxies are active galactic nuclei (AGN) displaying a bright core emission induced by accretion onto the central supermassive black hole (SMBH). Seyfert galaxies are non-jetted AGN, contrarily to radio galaxies such as Centaurus A, which can show prominent jets extending out to Mpc scales.
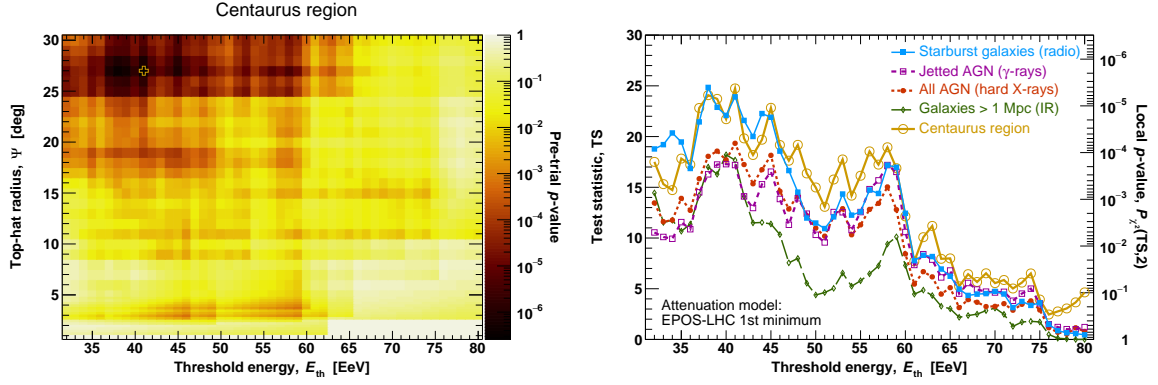
Figure 2: *Left*: The pre-trial *p*-value for an overdensity in the Centaurus region as a function of the energy threshold, E_{th}, and top-hat radius, Ψ. A golden cross marks the threshold energy and top-hat radius corresponding to the most significant signal. *Right*: The test statistic profile as a function of threshold energy for the four studied catalogs, with attenuation according to best-fit composition scenario from [13]. The local *p*-value, penalized for the search over the angular scale and signal fraction, is shown on the right-hand side axis. The profile of the local *p*-value for an overdensity in the Centaurus region, accounting for the scan in Ψ, is shown as a golden line.

　　Given the numerous objects which could contribute to the excess in the Centaurus region, we follow the analysis in [8] to determine whether specific flux patterns are preferred over the FoV of the Observatory. Four catalogs are investigated. The largest one, with 44,113 galaxies out to 250 Mpc and beyond the Local Group (> 1 Mpc), contains near-infrared (IR) observations from 2MASS up to a K-band magnitude of 11.75. We crossmatched the catalog with the HyperLEDA database,[5] which provides spectroscopic redshifts and cosmic-ladder distance estimates for galaxies out of the Hubble flow. This IR catalog, which is flux-limited over more than 90% of the sky and is essentially comparable to 2MRS, enables a mapping of stellar mass in the local Universe with appropriate distances for nearby objects. Galaxies with a high star-formation rate, loosely denoted here as "starburst" galaxies, are selected from [14]. We exclude from the original sample the LMC and the SMC which, as dwarf irregular galaxies, show a far-infrared ($60\,\mu$m) to radio (1.4 GHz) flux ratio higher by more than one order of magnitude with respect to starburst galaxies. We add to the sample the Circinus galaxy, as observed by the Parkes telescope, which was not included by [14] because of its location in the zone of avoidance. This compilation provides a sample of 44 starbursts with 1.4 GHz fluxes larger than 0.3 Jy between 1 and 130 Mpc, whose distances are extracted from HyperLEDA. Besides star formation, the other major process that can drive the life and feedback of a galaxy is AGN activity. Both non-jetted and jetted AGN are selected from the *Swift*-BAT 105-month catalog [15] with an integral flux between 14 and 195 keV larger than 8.4×10^{-12}erg s^{-1} cm^{-2} (flux limit over more than 90% of the sky). This X-ray sample, crossmatched with HyperLEDA and NED,[6] contains 523 AGNs between 1 and 250 Mpc. Finally, a specific attention is paid to jetted AGNs, selected from the *Fermi*-LAT 3FHL catalog [16] above a 10 GeV$-$1 TeV flux of 3.3×10^{-11} cm^{-2} s^{-1} (flux limit over 90% of the sky). A total of 26 sources remains after selection between 1 and 250 Mpc, with distances from HyperLEDA. These four catalogs are improved versions of those used in [8, 17], although the updates have negligible impact

---

[5]http://leda.univ-lyon1.fr/
[6]https://ned.ipac.caltech.edu/

Catalog	E_{th} [EeV]	Ψ [deg]	α [%]	TS	Post-trial p-value
All galaxies (IR)	40	24^{+16}_{-8}	15^{+10}_{-6}	18.2	6.7×10^{-4}
Starbursts (radio)	38	25^{+11}_{-7}	9^{+6}_{-4}	24.8	3.1×10^{-5}
All AGNs (X-rays)	41	27^{+14}_{-9}	8^{+5}_{-4}	19.3	4.0×10^{-4}
Jetted AGNs (γ-rays)	40	23^{+9}_{-8}	6^{+4}_{-3}	17.3	1.0×10^{-3}

Table 2: The results of the searches for anisotropies against catalogs. The second to fourth columns provide the threshold energy, the equivalent top-hat radius and the signal fraction maximizing the local TS, or post-trial p-value, shown in the fifth and sixth columns.

on the analysis results. The catalogs are fully complementary: 2MASS infrared observations of "all" galaxies provide, through stellar mass, a deep view on integrated star-formation activity; radio observations of bright starburst galaxies provide a more instantaneous view on ongoing starforming activity; X-ray observations provide a census of "all" active galaxies, be they jetted or non-jetted; γ-ray observations finally focus on a sub-sample of jetted active galaxies.

To determine whether the flux patterns from these catalogs contribute to the anisotropy in the toe region, we perform an unbinned maximum-likelihood ratio test [8] between the null hypothesis, isotropy, and the test hypothesis, that is a catalog contribution added to an isotropic component, where both hypotheses account for the exposure of the Observatory. The flux of each source is weighted according to the UHECR attenuation expected from the best-fit model of the spectral and composition data from [13]. The overall UHECR flux contribution of the catalog is normalized to a free amplitude α (that of the isotropic component is 1-α) and the catalog flux pattern is smoothed with a Fisher - von Mises function on a Gaussian angular scale, θ. The local test statistic, TS, corresponding to the maximum likelihood ratio is shown as a function of energy threshold in Fig. 2, right. The TS profiles of the catalogs display an energy dependence similar to that observed in the Centaurus region, obtained by profiling the pre-trial p-value in Fig. 2, left, and penalizing for the scan over the angular scale. As reported in Table 2, the signal is maximal for all four catalogs above an energy threshold close to 40 EeV. For the sake of comparison with other results, the best-fit Gaussian angular scales are converted to equivalent top-hat radii as $\Psi = 1.59 \times \theta$ [17], with best-fit values at $\Psi \approx 25°$. The signal fractions range from 6 to 15%. The local TS range between 17 and 25, yielding post-trial p-values between 10^{-3} ($3.1\,\sigma$) and 3×10^{-5} ($4.0\,\sigma$), accounting for the scan in energy threshold and the two free parameters (α, θ).

Although similar parameters are inferred for the four catalogs, the TS and corresponding post-trial p-values show marked differences. A quantitative comparison between the catalogs is performed, as in [8], by testing a composite model including contributions from catalog #1 and catalog #2 against a model including a contribution from catalog #1 only. A γ-ray only, X-ray only, or IR only contribution is disfavored with respect to a composite model including a radio contribution from starburst galaxies above $38 - 41$ EeV at confidence levels varying between 2 and $3\,\sigma$. While there is no significant indication for a preferred catalog, such differences can be qualitatively understood from a comparison of the observed flux map shown in Fig. 1 with the best-fit flux models shown in Fig. 3. The X-ray and γ-ray models of all and jetted AGNs are dominated by a contribution from Centaurus A, with additional mild contributions close to the edge of the FoV from NGC 4151 (so-called "Eye of Sauron") for the former and from the blazar Markarian 421 and the radio-galaxy NGC 1275 for the latter. The possible mild excess south of the edge of the
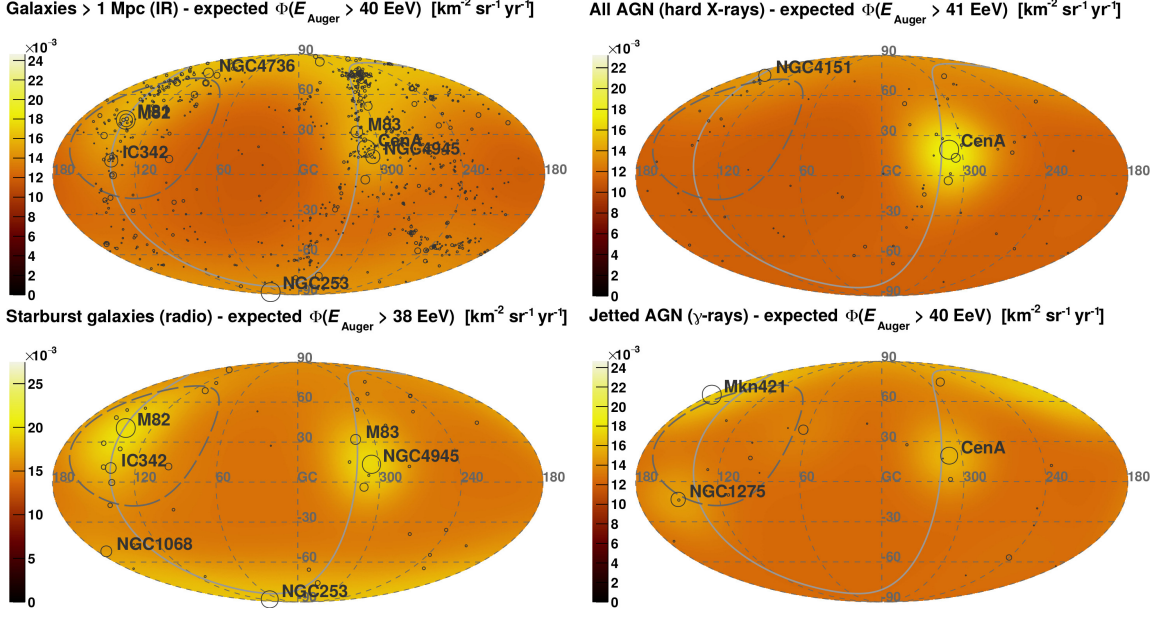
6

Figure 3: The best-fit flux models of the four catalogs in Galactic coordinates, smoothed on a top-hat scale of 24° as in Fig. 1. The maps are normalized so that the mean flux in the FoV of the Observatory equals the mean observed flux. The color scales cover the observed flux ranges above the best energy threshold associated to each catalog.

FoV in Fig. 1, which could be viewed as being associated to NGC 1275, is unlikely to contribute to the TS in any of the models as it arises from only few counts close to the edge of the FoV. The model of starburst galaxies features both a prominent excess in the Centaurus region, mostly from NGC 4945 and M 83, as well as an excess close to the South Galactic pole, dominated by NGC 253. This excess, together with a different pattern in the Centaurus region, is responsible for the larger TS score of the starburst model. The IR sky model shows prominent contributions both close to the South Galactic pole and in the Centaurus region, but the expected excess north of the latter region , arising from the Virgo cluster, appears to be disfavored by the observations.

4. Discussion and conclusion

UHECR observations at the Pierre Auger Observatory have enabled the firm detection of a large-scale anisotropy in the instep spectral region. This dipolar component provided the first observational evidence for UHECRs above the ankle originating outside the Milky Way. A total of 17 years of accumulated exposure further provides evidence for anisotropy in the toe region, on an angular scale of $\Psi \approx 25°$ (top-hat) or $\theta \approx 15°$ (Gaussian). Underconstrained searches, with no strong astrophysical *a priori*, are unable to catch any significant excess because of the vastness of the parameter space to be probed. A more constrained search based on early-day indications reveals a $\sim 5\%$ signal fraction from the Centaurus region. The evidence is confirmed up to a 4σ confidence level by analyses of UHECR arrival directions against multiwavelength catalogs tracing stellar mass, starforming activity, and AGN activity including or excluding non-jetted sources. The catalog yielding the smallest *p*-value grasps a possible tepid spot close to the South Galactic pole,

although no statistically compelling evidence for a catalog preference can be stated due to the limited event counts at the highest energies.

The observational ability to discriminate between extragalactic astrophysical scenarios nonetheless remains crucial: whether UHECR acceleration is linked to starforming or SMBH activity would point the community towards preferred sources, e.g. in the form of long γ-ray bursts or jetted AGNs, respectively. Such a potential may be offered by full-sky coverage, as illustrated by the different flux levels in the blind spot of the Observatory shown in Fig. 3. Probing mass composition across the celestial sphere may provide further clues, as different nuclear species probe different volumes of the Universe at a given energy. Finally, deeper multiwavelength catalogs of galaxies may provide a handle to model the UHECR sky from the ankle to the toe region. The combination of these efforts, explored separately in this proceeding volume, may very well provide answers to the seminal question of the field of astroparticles.

References

[1] A. Aab et al. [Pierre Auger Coll.], *Nucl. Instrum. Meth. A* **798** (2015) 172 [1502.01323].

[2] A. Aab et al. [Pierre Auger Coll.], *Phys. Rev. Lett.* **125** (2020) 121106 [2008.06488].

[3] A. Aab et al. [Pierre Auger Coll.], *Science* **357** (2017) 1266 [1709.07321].

[4] R. M. de Almeida [for the Pierre Auger Coll.], these proceedings.

[5] R. Aloisio, V. Berezinsky and S. Grigorieva, *Astropart. Phys.* **41** (2013) 94 [1006.2484].

[6] P. Erdoğdu, O. Lahav, J.P. Huchra et al., *Mon. Not. R. Astron. Soc.* **373** (2006) 45 [astro-ph/0610005].

[7] A. Aab et al. [Pierre Auger Coll.], *Astrophys. J.* **804** (2015) 15 [1411.6111].

[8] A. Aab et al. [Pierre Auger Coll.], *Astrophys. J. Lett.* **853** (2018) L29 [1801.06160].

[9] A. Aab et al. [Pierre Auger Coll.], *J. Instrum.* **15** (2020) P10021 [2007.09035].

[10] J. Biteau et al. [for the Pierre Auger and Telescope Array Coll.], *EPJ Web Conf.* **210** (2019) 01005 [1905.04188].

[11] A. Aab et al. [Pierre Auger Coll.], *Science* **318** (2007) 938 [0711.2256].

[12] M.L. McCall, *Mon. Not. R. Astron. Soc.* **440** (2014) 405 [1403.3667].

[13] A. Aab et al. [Pierre Auger Coll.], *J. Cosmol. Astropart. P.* **2017** (2017) 038 [1612.07155].

[14] C. Lunardini, G.S. Vance, K.L. Emig and R.A. Windhorst, *J. Cosmol. Astropart. P.* **2019** (2019) 073 [1902.09663].

[15] K. Oh, M. Koss, C.B. Markwardt et al., *Astrophys. J. Suppl. S.* **235** (2018) 4 [1801.01882].

[16] M. Ajello et al. [Fermi-LAT Coll.], *Astrophys. J. Suppl. S.* **232** (2017) 18 [1702.00664].

[17] L. Caccianiga [for the Pierre Auger Coll.], *Proc. 36th Int. Cosmic Ray Conf., Madison, USA (2019),* PoS(ICRC2019)206.

The Pierre Auger Collaboration
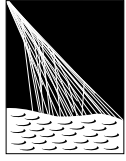
PIERRE
AUGER
OBSERVATORY

P. Abreu[71], M. Aglietta[53,51], J.M. Albury[12], I. Allekotte[1], A. Almela[8,11], J. Alvarez-Muñiz[78], R. Alves Batista[79], G.A. Anastasi[62,51], L. Anchordoqui[86], B. Andrada[8], S. Andringa[71], C. Aramo[49], P.R. Araújo Ferreira[41], J. C. Arteaga Velázquez[66], H. Asorey[8], P. Assis[71], G. Avila[10], A.M. Badescu[74], A. Bakalova[31], A. Balaceanu[72], F. Barbato[44,45], R.J. Barreira Luz[71], K.H. Becker[37], J.A. Bellido[12,68], C. Berat[35], M.E. Bertaina[62,51], X. Bertou[1], P.L. Biermann[b], V. Binet[6], K. Bismark[38,8], T. Bister[41], J. Biteau[36], J. Blazek[31], C. Bleve[35], M. Boháčová[31], D. Boncioli[56,45], C. Bonifazi[25], L. Bonneau Arbeletche[20], N. Borodai[69], A.M. Botti[8], J. Brack[d], T. Bretz[41], P.G. Brichetto Orchera[8], F.L. Briechle[41], P. Buchholz[43], A. Bueno[77], S. Buitink[14], M. Buscemi[46], M. Büsken[38,8], K.S. Caballero-Mora[65], L. Caccianiga[58,48], F. Canfora[79,80], I. Caracas[37], J.M. Carceller[77], R. Caruso[57,46], A. Castellina[53,51], F. Catalani[18], G. Cataldi[47], L. Cazon[71], M. Cerda[9], J.A. Chinellato[21], J. Chudoba[31], L. Chytka[32], R.W. Clay[12], A.C. Cobos Cerutti[7], R. Colalillo[59,49], A. Coleman[92], M.R. Coluccia[47], R. Conceição[71], A. Condorelli[44,45], G. Consolati[48,54], F. Contreras[10], F. Convenga[55,47], D. Correia dos Santos[27], C.E. Covault[84], S. Dasso[5,3], K. Daumiller[40], B.R. Dawson[12], J.A. Day[12], R.M. de Almeida[27], J. de Jesús[8,40], S.J. de Jong[79,80], G. De Mauro[79,80], J.R.T. de Mello Neto[25,26], I. De Mitri[44,45], J. de Oliveira[17], D. de Oliveira Franco[21], F. de Palma[55,47], V. de Souza[19], E. De Vito[55,47], M. del Río[10], O. Deligny[33], L. Deval[40], A. di Matteo[51], C. Dobrigkeit[21], J.C. D'Olivo[67], L.M. Domingues Mendes[71], R.C. dos Anjos[24], D. dos Santos[27], M.T. Dova[4], J. Ebr[31], R. Engel[38,40], I. Epicoco[55,47], M. Erdmann[41], C.O. Escobar[a], A. Etchegoyen[8,11], H. Falcke[79,81,80], J. Farmer[91], G. Farrar[89], A.C. Fauth[21], N. Fazzini[a], F. Feldbusch[39], F. Fenu[53,51], B. Fick[88], J.M. Figueira[8], A. Filipčič[76,75], T. Fitoussi[40], T. Fodran[79], M.M. Freire[6], T. Fujii[91,e], A. Fuster[8,11], C. Galea[79], C. Galelli[58,48], B. García[7], A.L. Garcia Vegas[41], H. Gemmeke[39], F. Gesualdi[8,40], A. Gherghel-Lascu[72], P.L. Ghia[33], U. Giaccari[79], M. Giammarchi[48], J. Glombitza[41], F. Gobbi[9], F. Gollan[8], G. Golup[1], M. Gómez Berisso[1], P.F. Gómez Vitale[10], J.P. Gongora[10], J.M. González[1], N. González[13], I. Goos[1,40], D. Góra[69], A. Gorgi[53,51], M. Gottowik[37], T.D. Grubb[12], F. Guarino[59,49], G.P. Guedes[22], E. Guido[51,62], S. Hahn[40,8], P. Hamal[31], M.R. Hampel[8], P. Hansen[4], D. Harari[1], V.M. Harvey[12], A. Haungs[40], T. Hebbeker[41], D. Heck[40], G.C. Hill[12], C. Hojvat[a], J.R. Hörandel[79,80], P. Horvath[32], M. Hrabovský[32], T. Huege[40,14], A. Insolia[57,46], P.G. Isar[73], P. Janecek[31], J.A. Johnsen[85], J. Jurysek[31], A. Kääpä[37], K.H. Kampert[37], N. Karastathis[40], B. Keilhauer[40], J. Kemp[41], A. Khakurdikar[79], V.V. Kizakke Covilakam[8,40], H.O. Klages[40], M. Kleifges[39], J. Kleinfeller[9], M. Köpke[38], N. Kunka[39], B.L. Lago[16], R.G. Lang[19], N. Langner[41], M.A. Leigui de Oliveira[23], V. Lenok[40], A. Letessier-Selvon[34], I. Lhenry-Yvon[33], D. Lo Presti[57,46], L. Lopes[71], R. López[63], L. Lu[93], Q. Luce[38], J.P. Lundquist[75], A. Machado Payeras[21], G. Mancarella[55,47], D. Mandat[31], B.C. Manning[12], J. Manshanden[42], P. Mantsch[a], S. Marafico[33], A.G. Mariazzi[4], I.C. Mariş[13], G. Marsella[60,46], D. Martello[55,47], S. Martinelli[40,8], O. Martínez Bravo[63], M. Mastrodicasa[56,45], H.J. Mathes[40], J. Matthews[87], G. Matthiae[61,50], E. Mayotte[37], P.O. Mazur[a], G. Medina-Tanco[67], D. Melo[8], A. Menshikov[39], K.-D. Merenda[85], S. Michal[32], M.I. Micheletti[6], L. Miramonti[58,48], S. Mollerach[1], F. Montanet[35], C. Morello[53,51], M. Mostafá[90], A.L. Müller[8], M.A. Muller[21], K. Mulrey[14], R. Mussa[51], M. Muzio[89], W.M. Namasaka[37], A. Nasr-Esfahani[37], L. Nellen[67], M. Niculescu-Oglinzanu[72], M. Niechciol[43], D. Nitz[88], D. Nosek[30], V. Novotny[30], L. Nožka[32], A Nucita[55,47], L.A. Núñez[29], M. Palatka[31], J. Pallotta[2], P. Papenbreer[37], G. Parente[78], A. Parra[63], J. Pawlowsky[37], M. Pech[31], F. Pedreira[78], J. Pękala[69], R. Pelayo[64], J. Peña-Rodriguez[29], E.E. Pereira Martins[38,8], J. Perez Armand[20], C. Pérez Bertolli[8,40], M. Perlin[8,40], L. Perrone[55,47], S. Petrera[44,45], T. Pierog[40], M. Pimenta[71], V. Pirronello[57,46], M. Platino[8], B. Pont[79], M. Pothast[80,79], P. Privitera[91], M. Prouza[31], A. Puyleart[88], S. Querchfeld[37], J. Rautenberg[37], D. Ravignani[8], M. Reininghaus[40,8], J. Ridky[31], F. Riehn[71], M. Risse[43], V. Rizi[56,45], W. Rodrigues de Carvalho[20], J. Rodriguez Rojo[10], M.J. Roncoroni[8], S. Rossoni[42], M. Roth[40], E. Roulet[1], A.C. Rovero[5], P. Ruehl[43], S.J. Saffi[12], A. Saftoiu[72], F. Salamida[56,45], H. Salazar[63], G. Salina[50], J.D. Sanabria Gomez[29], F. Sánchez[8], E.M. Santos[20], E. Santos[31], F. Sarazin[85], R. Sarmento[71], C. Sarmiento-Cano[8],

R. Sato[10], P. Savina[55,47,33], C.M. Schäfer[40], V. Scherini[47], H. Schieler[40], M. Schimassek[38,8], M. Schimp[37], F. Schlüter[40,8], D. Schmidt[38], O. Scholten[83,14], P. Schovánek[31], F.G. Schröder[92,40], S. Schröder[37], J. Schulte[41], S.J. Sciutto[4], M. Scornavacche[8,40], A. Segreto[52,46], S. Sehgal[37], R.C. Shellard[15], G. Sigl[42], G. Silli[8,40], O. Sima[72,f], R. Šmída[91], P. Sommers[90], J.F. Soriano[86], J. Souchard[35], R. Squartini[9], M. Stadelmaier[40,8], D. Stanca[72], S. Stanič[75], J. Stasielak[69], P. Stassi[35], A. Streich[38,8], M. Suárez-Durán[13], T. Sudholz[12], T. Suomijärvi[36], A.D. Supanitsky[8], Z. Szadkowski[70], A. Tapia[28], C. Taricco[62,51], C. Timmermans[80,79], O. Tkachenko[40], P. Tobiska[31], C.J. Todero Peixoto[18], B. Tomé[71], Z. Torrès[35], A. Travaini[9], P. Travnicek[31], C. Trimarelli[56,45], M. Tueros[4], R. Ulrich[40], M. Unger[40], L. Vaclavek[32], M. Vacula[32], J.F. Valdés Galicia[67], L. Valore[59,49], E. Varela[63], A. Vásquez-Ramírez[29], D. Veberič[40], C. Ventura[26], I.D. Vergara Quispe[4], V. Verzi[50], J. Vicha[31], J. Vink[82], S. Vorobiov[75], H. Wahlberg[4], C. Watanabe[25], A.A. Watson[c], M. Weber[39], A. Weindl[40], L. Wiencke[85], H. Wilczyński[69], M. Wirtz[41], D. Wittkowski[37], B. Wundheiler[8], A. Yushkov[31], O. Zapparrata[13], E. Zas[78], D. Zavrtanik[75,76], M. Zavrtanik[76,75], and L. Zehrer[75]

—————— • ——————

[1] Centro Atómico Bariloche and Instituto Balseiro (CNEA-UNCuyo-CONICET), San Carlos de Bariloche, Argentina

[2] Centro de Investigaciones en Láseres y Aplicaciones, CITEDEF and CONICET, Villa Martelli, Argentina

[3] Departamento de Física and Departamento de Ciencias de la Atmósfera y los Océanos, FCEyN, Universidad de Buenos Aires and CONICET, Buenos Aires, Argentina

[4] IFLP, Universidad Nacional de La Plata and CONICET, La Plata, Argentina

[5] Instituto de Astronomía y Física del Espacio (IAFE, CONICET-UBA), Buenos Aires, Argentina

[6] Instituto de Física de Rosario (IFIR) – CONICET/U.N.R. and Facultad de Ciencias Bioquímicas y Farmacéuticas U.N.R., Rosario, Argentina

[7] Instituto de Tecnologías en Detección y Astropartículas (CNEA, CONICET, UNSAM), and Universidad Tecnológica Nacional – Facultad Regional Mendoza (CONICET/CNEA), Mendoza, Argentina

[8] Instituto de Tecnologías en Detección y Astropartículas (CNEA, CONICET, UNSAM), Buenos Aires, Argentina

[9] Observatorio Pierre Auger, Malargüe, Argentina

[10] Observatorio Pierre Auger and Comisión Nacional de Energía Atómica, Malargüe, Argentina

[11] Universidad Tecnológica Nacional – Facultad Regional Buenos Aires, Buenos Aires, Argentina

[12] University of Adelaide, Adelaide, S.A., Australia

[13] Université Libre de Bruxelles (ULB), Brussels, Belgium

[14] Vrije Universiteit Brussels, Brussels, Belgium

[15] Centro Brasileiro de Pesquisas Fisicas, Rio de Janeiro, RJ, Brazil

[16] Centro Federal de Educação Tecnológica Celso Suckow da Fonseca, Nova Friburgo, Brazil

[17] Instituto Federal de Educação, Ciência e Tecnologia do Rio de Janeiro (IFRJ), Brazil

[18] Universidade de São Paulo, Escola de Engenharia de Lorena, Lorena, SP, Brazil

[19] Universidade de São Paulo, Instituto de Física de São Carlos, São Carlos, SP, Brazil

[20] Universidade de São Paulo, Instituto de Física, São Paulo, SP, Brazil

[21] Universidade Estadual de Campinas, IFGW, Campinas, SP, Brazil

[22] Universidade Estadual de Feira de Santana, Feira de Santana, Brazil

[23] Universidade Federal do ABC, Santo André, SP, Brazil

[24] Universidade Federal do Paraná, Setor Palotina, Palotina, Brazil

[25] Universidade Federal do Rio de Janeiro, Instituto de Física, Rio de Janeiro, RJ, Brazil

[26] Universidade Federal do Rio de Janeiro (UFRJ), Observatório do Valongo, Rio de Janeiro, RJ, Brazil

[27] Universidade Federal Fluminense, EEIMVR, Volta Redonda, RJ, Brazil

[28] Universidad de Medellín, Medellín, Colombia

[29] Universidad Industrial de Santander, Bucaramanga, Colombia

[30] Charles University, Faculty of Mathematics and Physics, Institute of Particle and Nuclear Physics, Prague, Czech Republic

[31] Institute of Physics of the Czech Academy of Sciences, Prague, Czech Republic

[32] Palacky University, RCPTM, Olomouc, Czech Republic

[33] CNRS/IN2P3, IJCLab, Université Paris-Saclay, Orsay, France

[34] Laboratoire de Physique Nucléaire et de Hautes Energies (LPNHE), Sorbonne Université, Université de Paris, CNRS-IN2P3, Paris, France

[35] Univ. Grenoble Alpes, CNRS, Grenoble Institute of Engineering Univ. Grenoble Alpes, LPSC-IN2P3, 38000 Grenoble, France

[36] Université Paris-Saclay, CNRS/IN2P3, IJCLab, Orsay, France

[37] Bergische Universität Wuppertal, Department of Physics, Wuppertal, Germany

[38] Karlsruhe Institute of Technology (KIT), Institute for Experimental Particle Physics, Karlsruhe, Germany

[39] Karlsruhe Institute of Technology (KIT), Institut für Prozessdatenverarbeitung und Elektronik, Karlsruhe, Germany

[40] Karlsruhe Institute of Technology (KIT), Institute for Astroparticle Physics, Karlsruhe, Germany

[41] RWTH Aachen University, III. Physikalisches Institut A, Aachen, Germany

[42] Universität Hamburg, II. Institut für Theoretische Physik, Hamburg, Germany

[43] Universität Siegen, Department Physik – Experimentelle Teilchenphysik, Siegen, Germany

[44] Gran Sasso Science Institute, L'Aquila, Italy

[45] INFN Laboratori Nazionali del Gran Sasso, Assergi (L'Aquila), Italy

[46] INFN, Sezione di Catania, Catania, Italy

[47] INFN, Sezione di Lecce, Lecce, Italy

[48] INFN, Sezione di Milano, Milano, Italy

[49] INFN, Sezione di Napoli, Napoli, Italy

[50] INFN, Sezione di Roma "Tor Vergata", Roma, Italy

[51] INFN, Sezione di Torino, Torino, Italy

[52] Istituto di Astrofisica Spaziale e Fisica Cosmica di Palermo (INAF), Palermo, Italy

[53] Osservatorio Astrofisico di Torino (INAF), Torino, Italy

[54] Politecnico di Milano, Dipartimento di Scienze e Tecnologie Aerospaziali , Milano, Italy

[55] Università del Salento, Dipartimento di Matematica e Fisica "E. De Giorgi", Lecce, Italy

[56] Università dell'Aquila, Dipartimento di Scienze Fisiche e Chimiche, L'Aquila, Italy

[57] Università di Catania, Dipartimento di Fisica e Astronomia, Catania, Italy

[58] Università di Milano, Dipartimento di Fisica, Milano, Italy

[59] Università di Napoli "Federico II", Dipartimento di Fisica "Ettore Pancini", Napoli, Italy

[60] Università di Palermo, Dipartimento di Fisica e Chimica "E. Segrè", Palermo, Italy

[61] Università di Roma "Tor Vergata", Dipartimento di Fisica, Roma, Italy

[62] Università Torino, Dipartimento di Fisica, Torino, Italy

[63] Benemérita Universidad Autónoma de Puebla, Puebla, México

[64] Unidad Profesional Interdisciplinaria en Ingeniería y Tecnologías Avanzadas del Instituto Politécnico Nacional (UPIITA-IPN), México, D.F., México

[65] Universidad Autónoma de Chiapas, Tuxtla Gutiérrez, Chiapas, México

[66] Universidad Michoacana de San Nicolás de Hidalgo, Morelia, Michoacán, México

[67] Universidad Nacional Autónoma de México, México, D.F., México

[68] Universidad Nacional de San Agustin de Arequipa, Facultad de Ciencias Naturales y Formales, Arequipa, Peru

[69] Institute of Nuclear Physics PAN, Krakow, Poland

[70] University of Łódź, Faculty of High-Energy Astrophysics,Łódź, Poland

[71] Laboratório de Instrumentação e Física Experimental de Partículas – LIP and Instituto Superior Técnico – IST, Universidade de Lisboa – UL, Lisboa, Portugal

[72] "Horia Hulubei" National Institute for Physics and Nuclear Engineering, Bucharest-Magurele, Romania

[73] Institute of Space Science, Bucharest-Magurele, Romania

[74] University Politehnica of Bucharest, Bucharest, Romania

[75] Center for Astrophysics and Cosmology (CAC), University of Nova Gorica, Nova Gorica, Slovenia

[76] Experimental Particle Physics Department, J. Stefan Institute, Ljubljana, Slovenia

[77] Universidad de Granada and C.A.F.P.E., Granada, Spain

[78] Instituto Galego de Física de Altas Enerxías (IGFAE), Universidade de Santiago de Compostela, Santiago de Compostela, Spain

[79] IMAPP, Radboud University Nijmegen, Nijmegen, The Netherlands

[80] Nationaal Instituut voor Kernfysica en Hoge Energie Fysica (NIKHEF), Science Park, Amsterdam, The Netherlands

[81] Stichting Astronomisch Onderzoek in Nederland (ASTRON), Dwingeloo, The Netherlands

[82] Universiteit van Amsterdam, Faculty of Science, Amsterdam, The Netherlands

[83] University of Groningen, Kapteyn Astronomical Institute, Groningen, The Netherlands

[84] Case Western Reserve University, Cleveland, OH, USA

[85] Colorado School of Mines, Golden, CO, USA

[86] Department of Physics and Astronomy, Lehman College, City University of New York, Bronx, NY, USA

[87] Louisiana State University, Baton Rouge, LA, USA

[88] Michigan Technological University, Houghton, MI, USA

[89] New York University, New York, NY, USA

[90] Pennsylvania State University, University Park, PA, USA

[91] University of Chicago, Enrico Fermi Institute, Chicago, IL, USA

[92] University of Delaware, Department of Physics and Astronomy, Bartol Research Institute, Newark, DE, USA

[93] University of Wisconsin-Madison, Department of Physics and WIPAC, Madison, WI, USA

——

[a] Fermi National Accelerator Laboratory, Fermilab, Batavia, IL, USA

[b] Max-Planck-Institut für Radioastronomie, Bonn, Germany

[c] School of Physics and Astronomy, University of Leeds, Leeds, United Kingdom

[d] Colorado State University, Fort Collins, CO, USA

[e] now at Hakubi Center for Advanced Research and Graduate School of Science, Kyoto University, Kyoto, Japan

[f] also at University of Bucharest, Physics Department, Bucharest, Romania